

# Benzyl Complexes of Lanthanide(II) and Lanthanide(III) Metals: Trends and Comparisons

Sjoerd Harder<sup>a</sup>, Christian Ruspic<sup>a</sup>, Nollaig Ní Bhriain<sup>b</sup>, Frederic Berkermann<sup>a</sup>, and Markus Schürmann<sup>c</sup>

<sup>a</sup> Universität Duisburg-Essen, Universitätsstraße 5, 45117 Essen, Germany

<sup>b</sup> Dow Benelux, Terneuzen, Netherlands

<sup>c</sup> Technische Universität Dortmund, Otto-Hahn-Straße 6, 44221 Dortmund, Germany

Reprint requests to Prof. Dr. S. Harder. E-mail: sjoerd.harder@uni-due.de

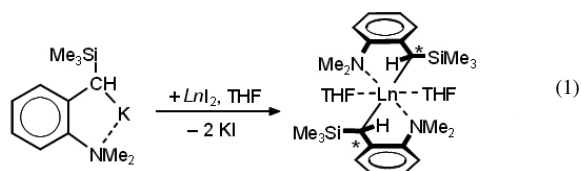
Z. Naturforsch. 2008, 63b, 267–274; received December 1, 2007

A variety of benzyllanthanide complexes have been prepared by the metathesis reaction of benzylpotassium precursors with lanthanide halides. Syntheses and crystal structures for the following complexes are described: [2-Me<sub>2</sub>N- $\alpha$ -Me<sub>3</sub>Si-benzyl]<sub>2</sub>Eu(II)·(THF)<sub>2</sub> (**1-Eu**), (2-Me<sub>2</sub>N-benzyl)<sub>3</sub>Ln(III) (**2-Ln** with Ln = Nd, Sm, Dy, Ho, Yb), (4-R-C<sub>6</sub>H<sub>4</sub>CH<sub>2</sub>)<sub>3</sub>Ln·(THF)<sub>3</sub> (**3-Y**: Ln = Y, R = H; **3-La**: Ln = La, R = *t*Bu). Complexes of types **1** and **2** are thermally robust on account of a stabilization by a benzylic Me<sub>3</sub>Si substituent and/or intramolecular coordination of the Me<sub>2</sub>N substituent. Comparison of the crystal structures of these new series of lanthanide complexes shows several similarities and trends. In addition, comparisons with alkali metal and alkaline earth metal benzyl complexes are made.

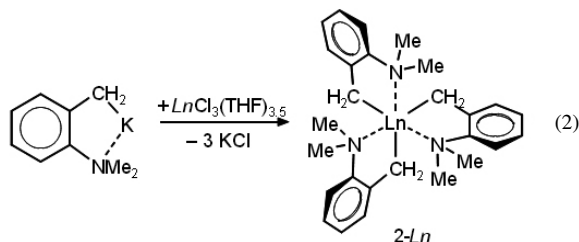
**Key words:** Benzyl Complexes, Lanthanide(II) Metal Complexes, Lanthanide(III) Metal Complexes, Crystal Structures

## Introduction

Some years ago, we reported syntheses and structures of the first homoleptic benzyl complexes of lanthanide metals in their less stable 2+ oxidation state (**1-Yb** and **1-Sm**, Eq. 1, Ln = lanthanide) [1]. The rather large coordination spheres of the Ln(II) centers are shielded by intramolecularly chelating Me<sub>2</sub>N substituents and the bulky Me<sub>3</sub>Si substituents in  $\alpha$ -position. As organometallic Ln(II) complexes display a high degree of ionicity in the Ln–C bond, the silyl substituent adds significantly to the stability of such compounds.

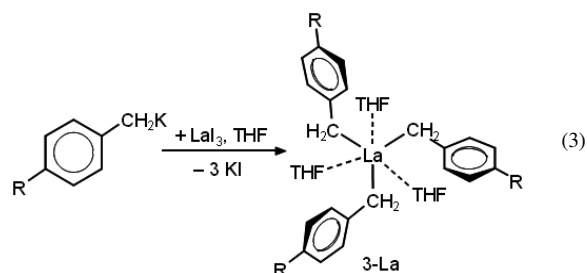


The first homoleptic Sc(III) benzyl complex had been introduced at an early stage by Manzer *et al.* [2] (**2-Sc** in Eq. 2). We reported a simple procedure for the syntheses of analogous homoleptic benzyllanthanide(III) complexes (Eq. 2) [3]. These complexes, which are stabilized by an intramolecular chelating



Me<sub>2</sub>N substituent in *ortho*-position, could not only be obtained for the small Y<sup>3+</sup> ion (ionic radius, 6-coordinate: 0.900 Å [4]) but also for the largest Ln<sup>3+</sup> ion La<sup>3+</sup> (1.032 Å). As **2-Y** and **2-La** crystallize isomorphously, it was anticipated that the new synthetic route and crystallization procedure are valid for the whole lanthanide series [3]. It was also shown that even the less reactive yttrium complex is a potent deprotonating reagent and a convenient starting material in lanthanide chemistry.

Subsequent work of the Hessen group [5] showed that simple *tris*-benzyl lanthanum complexes without intramolecular chelating amino substituents (**3-La** in Eq. 3) are available *via* the same synthetic route. The lanthanum complexes crystallize as *tris*-THF adducts and display similar octahedral metal coordination geometries as observed for **2-Y** and **2-La**.



Here we report new benzyl complexes of types **1–3** and discuss trends in their crystal structures and physical data. In addition, comparisons with alkali metal and alkaline earth metal benzyl complexes are made.

## Results and Discussion

### Syntheses and crystal structures

The dibenzyl Eu(II) complex **1-Eu** could be obtained in pure crystalline form (93 %) according to the metathesis route in Eq. 1. **1-Eu** represents the first benzyleuropium(II) complex and complements the series of other known homoleptic aryl, allyl, and alkyl-europium(II) compounds:  $(C_6F_5)_2Eu$  [6],  $[2,6-(Ph)_2C_6H_4]_2Eu$  [7],  $[1,3-(Me_3Si)_2-allyl]_2Eu$  [8] and  $[(Me_3Si)_3C]_2Eu$  [9]. On account of the high deprotonating power of the benzyl anion it is anticipated that this complex is a convenient precursor for the syntheses of a large variety of Eu(II) compounds.

Complex **1-Eu** crystallizes as an asymmetric *R/S* diastereomer (Fig. 1). The 2- $Me_2N$ - $\alpha$ - $Me_3Si$ -benzyl ligand coordinates to Eu as a bidentate C, N ligand with average C–Eu and N–Eu bond lengths of 2.772(3) Å and 2.779(3) Å, respectively. In contrast to the structure of **1-Yb**, the somewhat larger  $Eu^{2+}$  in **1-Eu** also shows short contacts to the aryl ring with Eu–C bond lengths varying from 2.833(2) to 2.939(3) Å. The crystal structure of **1-Eu** is isomorphous to those of **1-Sm** [1] and **1-Sr** [10]. The remarkably good agreement of the crystal structures (Fig. 1b) is due to very similar ionic radii for  $Eu^{2+}$  (8-coordinate: 1.17 Å),  $Sm^{2+}$  (1.22 Å) and  $Sr^{2+}$  (1.18 Å) [4].

In order to prove the generality of our previously reported synthetic route to (2- $Me_2N$ -benzyl) $_3Ln$ (III) complexes (**2-Ln**), we prepared the following complexes in crystalline purity: **2-Nd**, **2-Sm**, **2-Ho**, **2-Dy** and **2-Yb** (Eq. 2). All compounds show excellent solubility in aromatic solvents and are remarkably stable towards thermal decomposition. Toluene solutions of these homoleptic compounds can be stored at r. t. for more than four months with only negligible decompo-

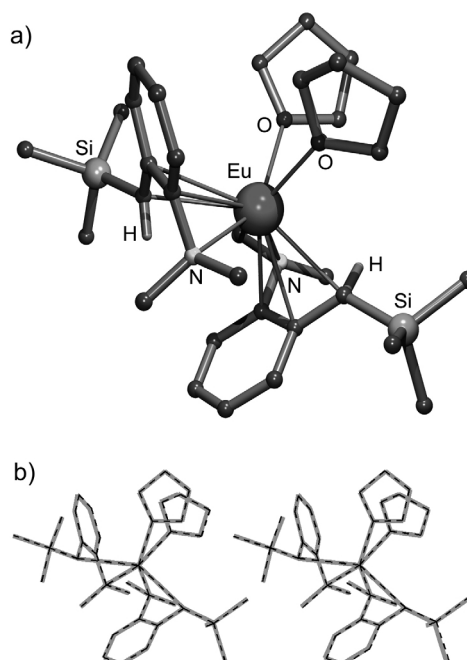


Fig. 1. (a) Crystal structure of **1-Eu**. Hydrogen atoms are not shown for clarity except the benzylic hydrogen atoms, which were located and refined. Geometrical parameters are given in Table 1. (b) Comparison of the crystal structures of **1-Eu** (thick grey lines) with that of **1-Sm** (striped black lines, left) and that of **1-Sr** (striped black lines, right).

sition (*ca.* 3 % *o*- $Me_2N$ -toluene is observed). Solutions can also be heated to 75 °C with only minor decomposition (*ca.* 5 % *o*- $Me_2N$ -toluene was observed after heating overnight). The advantageous stability of **2-Ln** complexes is likely due to the intramolecular coordination of the  $Me_2N$  substituents.

As expected, all complexes crystallize isomorphous to **2-Y** and **2-La**: the crystal structures show the typical paddle-wheel geometry (Fig. 2) with prismatic metal coordination. The threefold symmetry is broken by “up-side down” coordination of one of the bidentate benzyl ligands. The  $Ln$ –C and  $Ln$ –N bond lengths nicely correlate with the ionic radii for the  $Ln^{3+}$  ions (*vide infra*: trends and comparisons).

The series of unstabilized *tris*-benzylanthanide complexes has been extended with the synthesis and crystal structure of the yttrium(III) complex **3-Y** ( $R = H$ ). In addition, the new lanthanum(III) complex **3-La** ( $R = tBu$ ) has been prepared. The *tBu* substituents in the latter complex were introduced for higher solubility in apolar solvents. The solubilities in aromatic solvents and the thermal stabilities of **3-Y** and **3-La** are much lower than those of the  $Me_2N$ -stabilized series **2-Ln**.

Table 1. Selected bond lengths (Å), angles (deg) and NMR parameters for benzyllanthanide(II) and alkaline earth metal complexes of type **1-M**. A comparison is also made with the structures of the analogous Li and K compounds.

<b>1-M</b>	<b>Ca</b>	<b>Yb</b>	<b>Eu</b>	<b>Sr</b>	<b>Sm</b>	<b>Li<sup>a</sup></b>	<b>K<sup>b</sup></b>
Ionic radius <sup>c</sup>	1.12	1.14	1.25	1.26	1.27	0.92	1.51
Average M–C <sub>α</sub>	2.628(3)	2.651(3)	2.772(3)	2.781(2)	2.779(3)	2.219(6)	2.966(4)
Average M–N	2.600(2)	2.614(3)	2.757(2)	2.771(2)	2.764(2)	2.143(7)	2.906(3)
Average M–O	2.407(2)	2.454(3)	2.554(2)	2.546(2)	2.564(2)	–	2.633(4)
Average M···C <sub>ring</sub> <sup>d</sup>	3.095(3)	3.089(3)	2.902(3)	2.927(2)	2.904(2)	2.435(6)	3.163(3)
C <sub>α</sub> –Ln–N	67.1(1)	67.1(1)	62.7(1)	62.6(1)	62.7(1)	82.8(2)	59.5(1)
Average C <sub>α</sub> –C <sub>ipso</sub>	1.449(3)	1.443(5)	1.435(4)	1.430(3)	1.434(4)	1.426(4)	1.403(4)
C <sub>ortho</sub> –C <sub>α</sub> –C <sub>ortho</sub>	113.9(2)	113.9(3)	114.3(2)	114.2(2)	114.4(3)	114.2(3)	113.4(3)
Σ[C <sub>α</sub>	344(1)	346(1)	349(1)	350(1)	349(1)	358(1)	360(1)
<sup>1</sup> J <sub>C–H</sub> (Hz)	116	117	–	120	–	123	132
δ <sup>1</sup> H <sub>para</sub> (ppm)	6.33	6.36	–	6.29	–	6.29	5.78
δ <sup>13</sup> C <sub>para</sub> (ppm)	112.4	112.4	–	110.8	–	107.0	102.7

<sup>a</sup> Data for the Li analog 2-Me<sub>2</sub>N- $\alpha$ -Me<sub>3</sub>Si-benzyllithium·(TMEDA) [10]; <sup>b</sup> data for the K analog 2-Me<sub>2</sub>N- $\alpha$ -Me<sub>3</sub>Si-benzylpotassium·(THF) [10]; <sup>c</sup> ionic radii for 8-coordinate metal ions (Å) [4]; <sup>d</sup> average contacts to the two ring atoms: C<sub>ipso</sub> and C<sub>ortho</sub>.

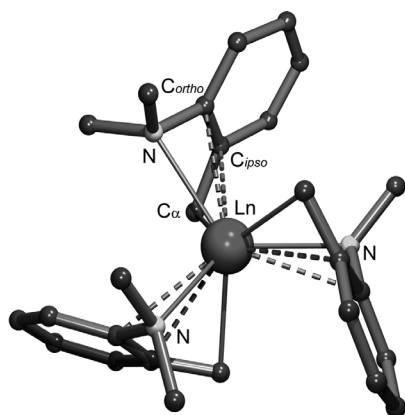


Fig. 2. General structural motif for the series **2-Ln** (shown here for **2-Nd**). Hydrogen atoms are not shown for clarity. Geometrical parameters are given in Table 2.

THF solutions gradually darken within hours already at r. t. After standing overnight, considerable quantities of toluene (or 4-*t*Bu-toluene) can be detected. Although the exact nature of the decomposition reaction could not be established, it has been proposed that carbene type intermediates like PhCH<sub>2</sub>Ln=CHPh are formed by  $\alpha$ -elimination [11].

The crystal structures of **3-Y** (R = H) and **3-La** (R = *t*Bu) could be determined (Fig. 3). Both, the Y and the La complex, crystallize similar to the earlier reported **3-La** (R = H) [5]. The distorted octahedral coordination environment with three benzyl groups in a facial arrangement is completed by three THF ligands. It is not clear why the negatively charged benzyl ligands are arranged in close proximity. It might be speculated that this preferred facial orientation can be explained by arguments similar to those used to rationalize the

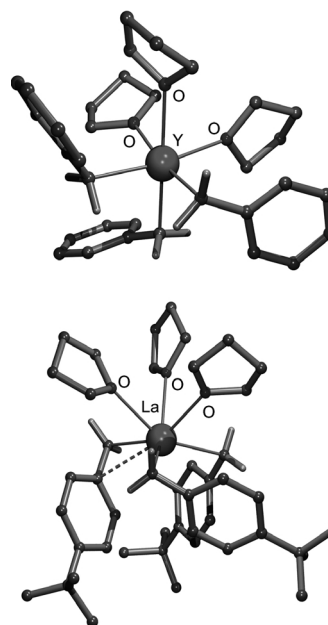


Fig. 3. Crystal structures of **3-Y** (R = H) and **3-La** (R = *t*Bu). Hydrogen atoms are not shown for clarity except the benzylic hydrogen atoms, which were located and refined. Geometrical parameters are given in Table 3.

unusual bent decametalocene structures of heavier alkaline earth and lanthanide metals [12]. Whereas the benzylic anions in **3-La** (R = *t*Bu) are partially bound in  $\eta^2$  fashion, those in **3-Y** (R = H) merely show  $\eta^1$  metal coordination.

#### Trends and comparisons

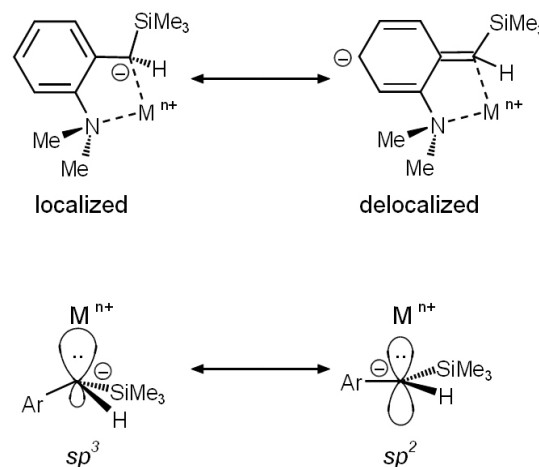
Three series of benzyllanthanide complexes are described. For each of these series, structural parameters

as a function of the metal are now available. This allows an evaluation of the metal effects on structure and bonding in benzylmetal chemistry.

For complexes of type **1**, comparisons can be made within the lanthanide series or with analogous heavier alkaline earth metal complexes which are known to be structurally similar [1]. Table 1 summarizes structural as well as NMR spectroscopic features in the series **1-Ca**, **1-Sr**, **1-Yb**, **1-Eu** and **1-Sm**. For sake of comparison, also data of alkali metal complexes based on the 2-Me<sub>2</sub>N- $\alpha$ -Me<sub>3</sub>Si-benzyl ligand have been included.

The M–C, M–N and M–O bond lengths increase with increasing ion size. Structural parameters for **1-Ca** show close similarities to those for **1-Yb** whereas the structure of **1-Sr** is very similar to the lanthanide complexes **1-Sm** and **1-Eu**. Increase of bond lengths with ion size is not proportional: the difference of 0.553 Å between the Eu–C bond and the shortest carbon metal bond, C–Li, is significantly larger than the difference of 0.32 Å in the ionic radii for Li and Eu.

The larger metals Eu, Sr, Sm and K display short interactions with two carbon atoms in the ring (*C<sub>ipso</sub>* and *C<sub>ortho</sub>*). The M··C<sub>ring</sub> bond lengths, defined as the average values of the M–*C<sub>ipso</sub>* and M–*C<sub>ortho</sub>* contacts, are between 4.5–6.6% longer than the M··C $\alpha$  bonds. For Ca and Yb much larger contacts are observed: the M··C<sub>ring</sub> distances are 16.5–17.8% longer than the C $\alpha$ ··metal contacts. Another obvious trend is the increase of the bite angle C $\alpha$ –M–N with increasing ion size. Also the effect of metal size on the delocalization of the negative charge from the benzylic carbon into the aryl ring can be observed. Two geometrical parameters are very sensitive to the extent of charge delocalization [3, 13]. First, the C $\alpha$ –C<sub>ipso</sub> bond length shortens on account of charge delocalization. All resonance structures, including the predominant resonance structure with a formal negative charge on the *para*-carbon atom (Scheme 1), display double bond character for the C $\alpha$ –C<sub>ipso</sub> bond. A second parameter sensitive towards charge delocalization is the endocyclic angle at C<sub>ipso</sub>. This angle is significantly squeezed with respect to an idealized *sp*<sup>2</sup> valence angle on account of charge delocalization. Analysis of these two parameters in Table 1 shows that: a) 2+ metal cations (Ca<sup>2+</sup>, Yb<sup>2+</sup>, Sr<sup>2+</sup>, Sm<sup>2+</sup>, Eu<sup>2+</sup>) localize the negative charge on the benzylic carbon whereas the weaker Lewis acids (Li<sup>+</sup> and K<sup>+</sup>) allow for significant charge delocalization and b) with respect to the larger congeners within a group, smaller cations (Ca<sup>2+</sup>, Yb<sup>2+</sup> and Li<sup>+</sup>) give rise to extensive charge localization.



Scheme 1.

These delocalization effects are also associated with the hybridization at the benzylic carbon atom. Although the determination of hydrogen positions in heavy atom X-ray diffraction structures should be taken with precaution, all benzylic hydrogen atoms have been located in the difference-Fourier maps and could be refined isotropically. This allows an evaluation of the hybridization of the benzylic carbon as a function of metal size and metal charge. The sum of the valence angles at the benzylic carbon atom (excluding angles involving the metal) is a measure for hybridization:  $\Sigma[C\alpha] \approx 328^\circ$  for *sp*<sup>3</sup> hybridization and  $360^\circ$  for *sp*<sup>2</sup> hybridization. The *sp*<sup>2</sup> character at the benzylic carbon atom increases with increasing metal size and decreasing metal charge (Table 1). The potassium complex 2-Me<sub>2</sub>N- $\alpha$ -Me<sub>3</sub>Si-benzylpotassium·(THF) [10] displays a perfectly planar benzylic carbon atom. As <sup>1</sup>J(C–H) NMR coupling constants are highly sensitive to hybridization effects, we also measured coupled <sup>13</sup>C NMR spectra for the diamagnetic complexes. The <sup>1</sup>J(C $\alpha$ –H) coupling constants increase with the extent of *s* character in the C–H bond, *i. e.* with increasing planarization of the benzylic carbon (Table 1). Thus, solution structures are in agreement with the geometrical parameters observed in the solid state structures. The chemical shifts of the *para*-carbon and *para*-hydrogen atoms are additional NMR probes for the evaluation of charge delocalization. An increased negative charge on the *para*-carbon atom generally results in a high-field shift of its NMR signals [13]. Decrease of chemical shift values with increasing extent of charge delocalization is indeed observed. Especially the potassium complex

Table 2. Selected bond lengths (Å) and angles (deg) for benzyllanthanide(III) complexes of type **2-Ln**.

<b>2-Ln</b>	<b>La</b>	<b>Nd</b>	<b>Sm</b>	<b>Dy</b>	<b>Ho</b>	<b>Y</b>	<b>Yb</b>
Ionic radius 6-coordinate (Å)	1.032	0.983	0.958	0.912	0.901	0.900	0.868
Average Ln–C <sub>α</sub>	2.645(3)	2.567(3)	2.531(4)	2.470(3)	2.476(3)	2.472(3)	2.419(3)
Average Ln–N	2.699(2)	2.647(2)	2.626(3)	2.577(2)	2.563(3)	2.566(3)	2.549(3)
Average M···C <sub>ring</sub> <sup>a</sup>	2.894(2)	2.855(3)	2.841(4)	2.828(2)	2.824(3)	2.822(3)	2.833(3)
C <sub>α</sub> –Ln–N	64.7(1)	66.2(1)	66.9(1)	68.5(1)	68.4(1)	68.8(1)	69.4(1)
Average C <sub>α</sub> –C <sub>ipso</sub>	1.432(4)	1.442(3)	1.438(5)	1.447(4)	1.432(4)	1.445(4)	1.454(5)
C <sub>ortho</sub> –C <sub>α</sub> –C <sub>ortho</sub>	115.0(2)	115.4(3)	114.9(3)	115.7(2)	115.4(3)	115.1(3)	115.5(3)

<sup>a</sup> Average contact to the two ring atoms C<sub>ipso</sub> and C<sub>ortho</sub>.

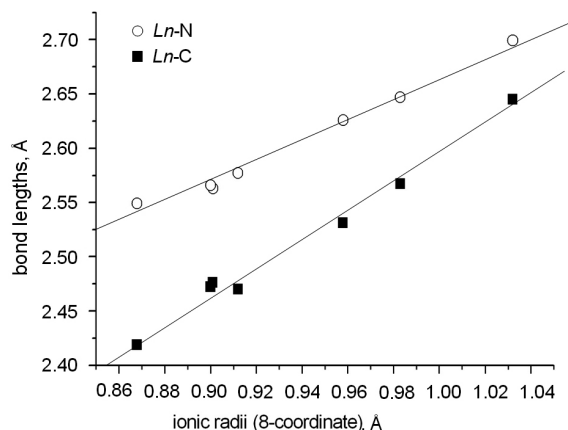


Fig. 4. Linear correlation between ionic radii and metal-ligand bond lengths in the series **2-Ln**.

shows very small chemical shifts for the *para*-H and C atoms.

Table 2 summarizes selected geometrical parameters for *tris*-(2-Me<sub>2</sub>N-benzyl)lanthanide complexes (**2-Ln**). The Ln–C<sub>α</sub> and Ln–N bonds increase linearly with increasing ion size (Fig. 4). The difference of 0.226(3) Å between the longest (Ln = La) and shortest (Ln = Yb) Ln–C<sub>α</sub> bond is somewhat larger than the difference of 0.164 Å in ionic radii of La and Yb. On the other hand, the difference of 0.150(3) Å between longest and shortest Ln–N bonds agrees well with the difference of 0.164 Å in ionic radii. The more distinct increase of Ln–C bond lengths with ion size is due to a more pronounced multihapto bonding for the larger lanthanide metals. Table 2 shows that the La···C<sub>ring</sub> distance in **2-La**, defined as the average value of La···C<sub>ipso</sub> and La···C<sub>ortho</sub>, is only 9.4% longer than the La–C<sub>α</sub> bond, whereas this difference increases to a value of 17.1% for **2-Yb**.

Another trend in the series is the observed increase in the C,N bite angle in going from the larger to the smaller metals. The two parameters associated with delocalization of negative charge from the benzylic

Table 3. Selected bond lengths (Å) and angles (deg) for benzyllanthanide(III) complexes of type **3-Ln**.

<b>3-Ln</b>	<b>3-Y</b> (R = H)	<b>3-La</b> (R = <i>t</i> Bu)	<b>3-La</b> (R = H) [5]	<b>3-La</b> (R = Me) [5]
Average Ln–C <sub>α</sub>	2.460(2)	2.633(2)	2.645(2)	2.626(2)
Average Ln–O	2.408(2)	2.672(2)	2.664(2)	2.692(2)
Average Ln···C <sub>ipso</sub>	3.387(3)	3.033(2)	2.978(2)	2.970(2)
Average C <sub>α</sub> –C <sub>ipso</sub>	1.466(2)	1.443(2)	1.436(3)	1.446(3)
Σ[C <sub>α</sub>	336(1)	345(2)	—	—

carbon C<sub>α</sub> into the ring (the bond length C<sub>α</sub>–C<sub>ipso</sub> and the endocyclic angle at C<sub>ipso</sub>) do not vary significantly along the series. However, comparison of these values for the largest metal ion (La<sup>3+</sup>) with those for the smallest metal ion (Yb<sup>3+</sup>) indeed confirms a slight decrease in charge delocalization with decreasing ion size. The benzylic hydrogen atoms could only be located in some of the crystal structures. Therefore, trends in the hybridization of the benzylic carbon atoms are not evaluated. As most Ln<sup>3+</sup> ions are paramagnetic, only NMR data for **2-La** and **2-Y** have been obtained [3]. The <sup>1</sup>J<sub>C–H</sub> value for C<sub>α</sub> in **2-La** (142.8 Hz) is significantly larger than that in **3-Y** (133.2 Hz). This confirms the less extensive charge delocalization (and concomitant pyramidalization of the benzylic carbon) in the latter complex.

Table 3 summarizes selected geometrical data for benzyllanthanide complexes of type **3-Ln**. The Ln–C and Ln–O bond lengths for the three La complexes compare well and are hardly influenced by alkyl substitution in *para*-position. Comparison of these bond lengths with those in **3-Y** (R = H) show that bonds to La are in general excessively long. Whereas the difference in ionic radii between La<sup>3+</sup> and Y<sup>3+</sup> is 0.132 Å, La–C and La–O bonds are on average 0.174(2) Å and 0.268 Å longer, respectively. This we attribute to more extensive Ln···C<sub>ipso</sub> interaction for the larger La atom. As can be deduced from a comparison of the C<sub>α</sub>–C<sub>ipso</sub> bond lengths, substituents in *para*-position hardly influence the extent of charge delocalization in the aryl ring. According to expectation, less extensive

charge delocalization is observed in **3-Y**. This corresponds to the more pyramidalized  $C_{\alpha}$  atom in **3-Y**.

## Conclusion

Benzyl complexes of the lanthanide metals have been routinely prepared by a simple protocol: the metathesis reaction of benzylpotassium precursors with the appropriate lanthanide halide. All benzyllanthanide complexes are powerful deprotonating agents and are therefore useful and easily accessible key precursors in *Ln*(II) as well as *Ln*(III) chemistry. Especially the robust, well-soluble complexes of type **2-Ln** are expected to become standard reagents in lanthanide chemistry. They are available for the whole lanthanide series (from the small Sc to the much larger La). Except for the Sc complex, for which hitherto no crystal structure is available, they all crystallize isomorphously and can be easily obtained in pure crystalline form.

The crystal structure of the benzylytterbium(II) complex **1-Yb** shows a striking similarity to that of the analogous calcium compound **1-Ca**. The *Ln*(II) complexes **1-Eu** and **1-Sm** are very similar to **1-Sr**. The structures show that charge delocalization into the aryl ring and  $Ln \cdots C_{\text{ring}}$  interactions increase with increasing metal size. Concomitant hybridization effects are observed at the benzylic carbon atoms. Similar trends are noticeable for the *Ln*(III) complexes of type **2-Ln** and **3-Ln**.

## Experimental Section

All manipulations were performed under a dry and oxygen-free atmosphere (argon or nitrogen) by using freshly dried solvents and Schlenk line and glove box techniques. The reactants 2-Me<sub>2</sub>N- $\alpha$ -Me<sub>3</sub>Si-benzylpotassium [10], 2-Me<sub>2</sub>N-benzylpotassium [14], 4-*t*Bu-benzylpotassium [15], EuI<sub>2</sub>·(THF)<sub>2</sub> [16], YCl<sub>3</sub>·(THF)<sub>3,5</sub> [17] and LaBr<sub>3</sub>·(THF)<sub>3,1</sub> [18] were prepared according to literature procedures.

### 1-Eu

A mixture of 2-Me<sub>2</sub>N- $\alpha$ -Me<sub>3</sub>Si-benzylpotassium (1.00 g, 4.07 mmol) and EuI<sub>2</sub>·(THF)<sub>2</sub> (1.10 g, 2.00 mmol) in 20 mL of THF was stirred in a glovebox for 40 h. After removing the solvent under high vacuum, the product was extracted with two 20 mL portions of benzene. Removing all solvents under vacuum gave an orange-red foam which was dissolved in a mixture of 15 mL of hexane and 8 mL of THF by heating to reflux temperature. Slow cooling of the orange solution to +4 °C gave well-formed orange needles of the paramagnetic product **1-Eu** with one equivalent of uncoordinated

THF in the crystal lattice. After isolation of the crystals the mother liquor was concentrated and cooled again. The combined fractions gave a yield of 1.45 g (93 %) – M. p. 168 °C (decomp.) – C<sub>36</sub>H<sub>64</sub>N<sub>2</sub>O<sub>3</sub>Si<sub>2</sub>Eu (781.06): calcd. C 55.36, H 8.26; found C 54.98, H 7.94.

### 2-Yb

A cooled solution (–50 °C) of 2.08 g (12.0 mmol) 2-Me<sub>2</sub>N- $\alpha$ -Me<sub>3</sub>Si-benzylpotassium in 20 mL of THF was added to a cooled slurry (–50 °C) of 1.12 g (4.01 mmol) YbCl<sub>3</sub> in 30 mL of THF. An immediate color change to dark blue was observed. The reaction mixture was allowed to warm up to r.t. and stirred for 1 h at 25 °C. After centrifugation the volatiles were evaporated under vacuum (25 °C, 1 Torr, 30 min), and the residue recrystallized from toluene/hexane in the form of dark blue blocks. Yield: 596 mg (26 %) – M. p. 157 °C (decomp.) – C<sub>27</sub>H<sub>36</sub>N<sub>3</sub>Yb (575.63): calcd. C 56.34, H 6.30; found C 56.01, H 6.42.

### 2-Sm

Same procedure as described for **2-Yb**, but with SmBr<sub>3</sub> instead of YbCl<sub>3</sub>. The product crystallized in the form of dark red blocks. Yield: 21 % – M. p. 150 °C (decomp.) – Despite its paramagnetic behavior reasonably well-resolved NMR spectra could be obtained (the assignments are tentative); <sup>1</sup>H NMR (300 MHz, C<sub>6</sub>D<sub>6</sub>):  $\delta$  = –1.77 (b, 18H, NMe<sub>2</sub>), 4.58 (b, 3H, aryl), 7.12 (b, 3H, aryl), 7.25 (b, 3H, aryl), 9.80 (b, 3H, aryl), 14.25 (b, 6H, CH<sub>2</sub>). – <sup>13</sup>C NMR (75 MHz, C<sub>6</sub>D<sub>6</sub>):  $\delta$  = 39.4 (NMe<sub>2</sub>), 44.7 (CH<sub>2</sub>), aromatics: 111.9, 122.7, 124.3, 128.7, 131.5, 154.7. – C<sub>27</sub>H<sub>36</sub>N<sub>3</sub>Sm (552.95): calcd. C 58.65, H 6.56; found C 58.23, H 6.62.

### 2-Nd

Same procedure as described for **2-Yb**, but with NdCl<sub>3</sub> instead of YbCl<sub>3</sub>. The product crystallized in the form of green-brown blocks. Yield: 32 % – M. p. 146 °C (decomp.) – C<sub>27</sub>H<sub>36</sub>N<sub>3</sub>Nd (546.83): calcd. C 59.30, H 6.64; found C 59.13, H 6.81.

### 2-Dy

Same procedure as described for **2-Yb** but with DyCl<sub>3</sub> instead of YbCl<sub>3</sub>. The product crystallized in the form of yellow blocks. Yield: 38 % – M. p. 154 °C (decomp.) – C<sub>27</sub>H<sub>36</sub>N<sub>3</sub>Dy (565.09): calcd. C 57.39, H 6.42; found C 57.05, H 6.59.

### 2-Ho

Same procedure as described for **2-Yb** but with HoCl<sub>3</sub> instead of YbCl<sub>3</sub>. The product crystallized in the form of orange blocks. Yield: 38 % – M. p. 156 °C (decomp.) – C<sub>27</sub>H<sub>36</sub>N<sub>3</sub>Ho (567.53): calcd. C 57.14, H 6.39; found C 56.79, H 6.29.

Table 4. Crystal structure data for **1-Eu**, **2-Nd**, **2-Sm**, **2-Dy**, **2-Ho**, **2-Yb**, **3-Y** ( $R = H$ ) and **3-La** ( $R = tBu$ ).

	<b>1-Eu</b>	<b>2-Nd</b>	<b>2-Sm</b>	<b>2-Dy</b>	<b>2-Ho</b>	<b>2-Yb</b>	<b>3-Y</b> ( $R = H$ )	<b>3-La</b> ( $R = tBu$ )
Formula	$C_{32}H_{56}O_2N_2Si_2Eu \cdot (C_4H_8O)$	$C_{27}H_{36}N_3Nd$	$C_{27}H_{36}N_3Sm$	$C_{27}H_{36}N_3Dy$	$C_{27}H_{36}N_3Ho$	$C_{27}H_{36}N_3Yb$	$C_{33}H_{45}O_3Y$	$C_{45}H_{69}O_3La \cdot (C_4H_8O)_2$
$M_r$	781.03	546.83	552.95	565.09	567.52	575.63	56578.60	941.12
Crystal system	triclinic	monoclinic	monoclinic	monoclinic	monoclinic	monoclinic	monoclinic	triclinic
Space group	$P\bar{1}$	$P2_1/c$	$P2_1/c$	$P2_1/c$	$P2_1/c$	$P2_1/c$	$Cc$	$P\bar{1}$
$a$ , Å	9.9253(7)	16.9666(8)	16.8989(8)	16.8456(6)	16.8083(6)	16.8969(5)	17.3879(9)	14.2601(4)
$b$ , Å	10.3021(8)	9.4546(5)	9.4648(7)	9.4500(3)	9.4614(3)	9.4642(3)	20.9547(10)	914.7473(4)
$c$ , Å	20.1525(12)	16.6784(10)	16.6603(10)	16.6181(5)	16.6151(4)	16.6694(5)	8.4526(4)	15.3114(5)
$\alpha$ , deg	85.728(6)	90	90	90	90	90	90	110.177(1)
$\beta$ , deg	89.639(5)	110.685(3)	110.911(3)	111.123(2)	111.217(2)	111.297(2)	93.286(3)	96.731(2)
$\gamma$ , deg	75.215(6)	90	90	90	90	90	90	115.043(1)
$V$ , Å <sup>3</sup>	1986.7(2)	2503.0(2)	2489.2(3)	2467.7(1)	2563.2(1)	2483.7(1)	2467.7(1)	2603.8(1)
$Z$	2	4	4	4	4	4	4	2
$D_{calcd}$ , g cm <sup>-3</sup>	1.306	1.451	1.475	1.521	1.530	1.539	1.250	1.200
$\mu$ (MoK $\alpha$ ), cm <sup>-1</sup>	1.672	2.092	2.377	3.046	3.230	3.783	1.926	0.862
$F(000)$ , e	818	1116	1124	1140	1144	1156	1124	1000
$T$ , K	203	173	173	173	173	203	203	203
$\theta_{max}$ , deg	27.1	27.5	27.5	27.5	27.5	27.6	35.5	30.0
Refl. measured	9216	27182	25069	24890	24756	48573	80223	135472
Refl. unique	8720	5713	5690	5645	5637	5761	11636	15059
Refl. $I \geq 2\sigma(I)$	8204	3559	2922	4613	4489	5092	9166	13317
$R_{int}$	0.014	0.035	0.042	0.041	0.035	0.052	0.065	0.034
Param. refined	592	286	286	305	280	402	358	584
$R(F)$	0.028	0.029	0.030	0.021	0.024	0.022	0.036	0.031
$wR(F^2)$ all	0.078	0.046	0.047	0.044	0.052	0.056	0.088	0.088
GoF ( $F^2$ )	1.08	0.80	0.66	0.99	1.00	1.11	1.00	1.07
$\Delta\rho_{min}$ (max/min), e Å <sup>-3</sup>	-1.15 / 1.16	-1.68 / 0.87	-1.92 / 0.95	-0.87 / 1.76	-0.98 / 1.63	-1.17 / 0.50	-0.84 / 0.51	-0.61 / 0.89

**3-Y** ( $R = H$ )

A cold dark-red solution ( $-50$  °C) of benzylpotassium (0.90 g, 6.91 mmol) in 20 mL of THF was added to  $YCl_3 \cdot (THF)_{3.5}$  (1.12 g, 4.01 mmol). An immediate color change to yellow-orange was observed, and a grey precipitate formed. After stirring for 30 min the mixture was concentrated to 50% of its original volume, and 10 mL of hexane was added. The yellow-white precipitate was isolated, and the product was extracted from this solid with two 20 mL portions of a THF/hexane mixture (1/1). The combined extracts were concentrated under high vacuum to 25% of their original volume, and the solution was slowly cooled to  $-30$  °C. The product was isolated in the form of light-yellow crystals (0.32 g, 24%) – M. p.  $136$  °C (decomp.) –  $^1H$  NMR (300 MHz,  $C_6D_6$ ):  $\delta = 1.17$  (m, 12H, THF), 1.75 (d,  $^2J(^1H-^{89}Y) = 2.1$  Hz, 6H,  $CH_2$ ), 3.40 (m, 12H, THF), 6.73 (m, 9H, aryl), 7.12 (m, 6H, aryl). –  $^{13}C$  NMR (75 MHz,  $C_6D_6$ ):  $\delta = 25.3$  (THF), 52.7 (d,  $^1J(^{13}C-^{89}Y) = 31.3$ ,  $CH_2$ ), 68.5 (THF), aromatics: 117.4, 123.2, 129.3, 151.8. –  $C_{33}H_{45}O_3Y$  (578.63): calcd. C 68.50, H 7.84; found C 68.06, H 7.81.

**3-La** ( $R = tBu$ )

A cold dark-red solution ( $-50$  °C) of 4-*t*Bu-benzylpotassium (1.00 g, 5.37 mmol) in 40 mL of

THF was added to  $LaBr_3 \cdot (THF)_{3.1}$  (1.07 g, 1.82 mmol). The resulting yellow suspension was stirred for 2 h at  $0$  °C. The mother liquor was separated from the precipitate by centrifugation and concentrated to 10 mL. The THF solution was layered carefully with 10 mL of pentane and slowly cooled to  $-30$  °C. The product was isolated in the form of orange crystals (0.36 g, 25%) – M. p.  $118$  °C (decomp.) –  $^1H$  NMR (300 MHz,  $[D_8]-THF$ ):  $\delta = 1.18$  (s, 27H, *t*Bu), 1.31 (s, 6H,  $CH_2$ ), 1.72 (m, 12H, THF), 3.57 (m, 12H, THF), 6.07 (d,  $J = 8.0$  Hz, 6H, aryl), 6.89 (d,  $J = 8.0$  Hz, 6H, aryl). –  $^{13}C$  NMR (75 MHz,  $[D_8]-THF$ ):  $\delta = 25.3$  (THF), 32.3 ( $Me_3C$ ), 34.2 ( $Me_3C$ ), 64.3 ( $CH_2$ ), 68.5 (THF), aromatics: 121.4, 127.4, 137.6, 149.0. –  $C_{45}H_{69}O_3La$  (796.95): calcd. C 67.82, H 8.73; found C 67.41, H 8.62.

*Crystal structure determinations*

The structures were solved by Direct Methods (SHELXS-97) [19] and refined with SHELXL-97 [20]. All geometry calculations and graphics were performed with PLATON [21]. Crystal data are summarized in Table 4.

CCDC 665306 (**2-Yb**), 665307 (**2-Sm**), 671057 (**3-La**), 671058 (**3-Y**), 671059 (**2-Dy**), 671060 (**2-Ho**), 671061 (**2-Nd**), 671062 (**1-Eu**) contain the supplementary crystallographic data for this paper. These data can be obtained free of charge from The Cambridge Crystallographic Data Centre via [http://www.ccdc.cam.ac.uk/data\\_request/cif](http://www.ccdc.cam.ac.uk/data_request/cif).

*Acknowledgements*

The Deutsche Forschungsgemeinschaft is acknowledged for support of this work within the SPP 1166 program. Prof. Dr. R. Boese and D. Bläser (Universität Duisburg-Essen) are thanked for the collection of part of the X-ray diffraction data.

- 
- [1] S. Harder, *Angew. Chem.* **2004**, *116*, 2768; *Angew. Chem. Int. Ed.* **2004**, *43*, 2714.
- [2] L. E. Manzer, *J. Am. Chem. Soc.* **1978**, *100*, 8068.
- [3] S. Harder, *Organometallics* **2005**, *24*, 373.
- [4] R. D. Shannon, *Acta Cryst.* **1976**, *A32*, 751.
- [5] S. Bambirra, A. Meetsma, B. Hessen, *Organometallics* **2006**, *25*, 3454.
- [6] G. B. Deacon, C. M. Forsyth, *Chem. Eur. J.* **2004**, *10*, 1798.
- [7] G. Heckmann, M. Niemeyer, *J. Am. Chem. Soc.* **2000**, *122*, 4227.
- [8] C. K. Simpson, R. E. White, C. N. Carlson, D. A. Wroblewski, C. J. Kühn, T. A. Croce, I. M. Steele, B. L. Scott, V. G. Young, T. P. Hanusa, *Organometallics* **2005**, *24*, 3685.
- [9] C. Eaborn, P. B. Hitchcock, K. Izod, Z.-R. Lu, J. D. Smith, *Organometallics* **1996**, *15*, 4783.
- [10] F. Feil, S. Harder, *Organometallics* **2001**, *20*, 4616.
- [11] a) I. S. Guzman, N. N. Chigir, O. K. Sharaev, G. N. Bondarenko, E. I. Tinyakova, B. A. Dolgoplosk, *Dokl. Akad. Nauk SSSR* **1979**, *249*, 860; b) N. N. Chigir, I. S. Guzman, O. K. Sharaev, E. I. Tinyakova, B. A. Dolgoplosk, *Dokl. Akad. Nauk SSSR* **1982**, *263*, 375.
- [12] a) R. A. Andersen, J. M. Boncella, C. J. Burns, R. Blom, A. Haaland, H. V. Volden, *J. Organomet. Chem.* **1986**, *312*, C49; b) R. A. Williams, T. P. Hanusa, J. C. Huffman, *Organometallics* **1990**, *9*, 1128; c) M. Kaupp, P. v. Schleyer, M. Dolg, H. Stoll, *J. Am. Chem. Soc.* **1992**, *114*, 8202; d) T. K. Hollis, J. K. Burdett, B. Bosnich, *Organometallics* **1993**, *12*, 3385; e) T. P. Hanusa, *Organometallics* **2002**, *21*, 2559; f) M. Schultz, C. J. Burns, D. J. Schwartz, R. A. Andersen, *Organometallics* **2002**, *21*, 2559; g) W. J. Evans, L. A. Hughes, T. P. Hanusa, *J. Am. Chem. Soc.* **1984**, *106*, 4270.
- [13] D. Hoffmann, W. Bauer, F. Hampel, N. J. R. van Eikema Hommes, P. von R. Schleyer, P. Otto, U. Pieper, D. Stalke, D. S. Wright, R. Snaith, *J. Am. Chem. Soc.* **1994**, *116*, 528.
- [14] S. Harder, F. Feil, *Organometallics* **2002**, *21*, 2268.
- [15] S. Harder, S. Müller, E. Hübner, *Organometallics* **2004**, *23*, 178.
- [16] P. Watson, T. H. Tulip, I. Williams, *Organometallics* **1990**, *9*, 1999.
- [17] P. Bruin, J. H. Booij, J. H. Teuben, A. Oskam, *J. Organomet. Chem.* **1988**, *350*, 17.
- [18] G. B. Deacon, T. Feng, P. C. Junk, G. Meyer, N. M. Scott, B. W. Skelton, A. White, *Austr. J. Chem.* **2000**, *53*, 853.
- [19] G. M. Sheldrick, SHELXS-97, Program for the Solution of Crystal Structures, University of Göttingen, Göttingen (Germany) **1997**.
- [20] G. M. Sheldrick, SHELXL-97, Program for the Refinement of Crystal Structures, University of Göttingen, Göttingen (Germany) **1997**.
- [21] A. L. Spek, PLATON, A Multipurpose Crystallographic Tool, Utrecht University, Utrecht (The Netherlands) **2000**. See also: A. L. Spek, *J. Appl. Cryst.* **2003**, *36*, 7–13.